



## Titanium doped silicon layers with very high concentration

J. Olea, M. Toledano-Luque, D. Pastor, G. González-Díaz, and I. Mártil

Citation: *Journal of Applied Physics* **104**, 016105 (2008); doi: 10.1063/1.2949258

View online: <http://dx.doi.org/10.1063/1.2949258>

View Table of Contents: <http://scitation.aip.org/content/aip/journal/jap/104/1?ver=pdfcov>

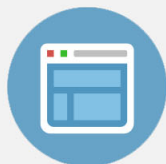
Published by the [AIP Publishing](#)

---



## Re-register for Table of Content Alerts

Create a profile.



Sign up today!



# Titanium doped silicon layers with very high concentration

J. Olea,<sup>a)</sup> M. Toledano-Luque, D. Pastor, G. González-Díaz, and I. Mártel

*Dpto. de Física Aplicada III (Electricidad y Electrónica), Facultad de Ciencias Físicas, Universidad Complutense de Madrid, Madrid E-28040, Spain*

(Received 18 March 2008; accepted 25 April 2008; published online 3 July 2008)

Ion implantation of Ti into Si at high doses has been performed. After laser annealing the maximum average of substitutional Ti atoms is about  $10^{18} \text{ cm}^{-3}$ . Hall effect measurements show  $n$ -type samples with mobility values of about  $400 \text{ cm}^2/\text{V s}$  at room temperature. These results clearly indicate that Ti solid solubility limit in Si has been exceeded by far without the formation of a titanium silicide layer. This is a promising result toward obtaining of an intermediate band into Si that allows the design of a new generation of high efficiency solar cell using Ti implanted Si wafers. © 2008 American Institute of Physics. [DOI: [10.1063/1.2949258](https://doi.org/10.1063/1.2949258)]

The formation of an intermediate band (IB) in the mid-gap of a semiconductor has shown potential for drastically improving the efficiency of single junction solar cells.<sup>1</sup> This approach permits electrons of energy below the band gap to be pumped from the valence band into conduction band via two-photon absorption of lower energy that use this IB as an intermediary step.

IB solar cells can be created in a semiconductor from deep level impurities if their concentration is high enough. Titanium (Ti) is a well known deep impurity in Si which introduces a donor level. For instance, a level at 0.22 eV below the conduction band has been detected by Hall effect experiments.<sup>2</sup> Although deep level transient spectroscopy studies pointed to a deeper position of the level (about 0.29 eV).<sup>3</sup> It is suggested that Ti atoms diffuse in silicon through a simple interstitial process according to electron paramagnetic resonance measurements of such samples.<sup>4</sup> These impurities are a well known source of nonradiative Shockley-Reed-Hall (SRH) recombination. However, it has been argued that this recombination may be suppressed when the Ti concentration is high enough as to exceed the Mott transition ( $5 \times 10^{19} \text{ cm}^{-3}$ ), and a band instead of a level of isolated impurities is formed.<sup>5</sup>

The aim of this communication is to show that the combination of different experimental techniques and the use of laser thermal processing allows the introduction of Ti atoms into the Si lattice in concentrations near or above the Mott limit, proving the possibility to form the IB in Si with this element.

Single crystal  $200 \Omega \text{ cm}$   $n$ -Si samples ( $\mu = 1250 \text{ cm}^2/\text{V s}$  and  $n = 2.2 \times 10^{13} \text{ cm}^{-3}$  measured at room temperature) were implanted with Ti ions by means of a VARIAN CF3000 ion implanter refurbished by IBS. Ti was implanted at 25 keV, with doses in the  $10^{15}$ – $5 \times 10^{16} \text{ cm}^{-2}$  range. Then, the implanted Si samples were laser annealed to activate Ti impurities. Annealing processes were carried out at J.P. Sercel Associates, Inc. (New Hampshire, USA) with a KrF excimer laser (248 nm) at energy densities from 0.2 to  $0.8 \text{ J/cm}^2$ , annealing with one or two pulses. Each pulse

lasted 20 ns. The implantation was previously simulated with Stopping Range of Ions in Matter code (SRIM). This simulation concluded that the thickness of the implanted layer was about 100 nm. The energy of implantation sites the maximum of the profile within the process window<sup>6</sup> using these energy densities, therefore all the Ti implanted is within the melted region during the annealing.

Time of flight secondary ion mass spectroscopy (ToF-SIMS) was used to obtain the Ti doping profile before and after the laser thermal processing. ToF-SIMS measurements were performed with a TOF\_SIMS IV model manufactured by ION-TOF.

The percentage of substitutional Ti incorporated into the silicon lattice was determined by Rutherford backscattering spectroscopy (RBS) and channeling-RBS measurements, using a tandem Cockcroft–Walton accelerator built by High Voltage Engineering Europe and working with 2 MeV He ions.

X-ray diffraction (XRD) was performed to study the crystallinity of the implanted layer using a Panalytical X'Pert PRO MRD diffractometer with Cu  $K\alpha$  radiation in glancing incidence configuration (GIXRD). This technique provides depth-resolved information about the crystal structure by means of the incidence angle of the x-ray source.<sup>7</sup>

Finally, Si implanted samples were electrically characterized by van der Pauw and Hall effect measurements at variable temperature using a Keithley SCS 4200 model, setting the sample inside a homemade variable temperature sample holder attached to a vacuum pump to avoid moisture condensation. Temperature varied between 90 and 380 K. A Kepco BOP 50–20MG bipolar power supply fed the electromagnet, reducing the thermo-galvanic-magnetic effects by changing the magnetic flux direction. Differential Hall effect algorithm was used to obtain both the dopant concentration and Hall mobility of the implanted layer by means of the following equations:<sup>8</sup>

$$\frac{1}{R_{S,\text{impl}}} - \frac{1}{R_{S,\text{subs}}} = q[n]_{\text{layer}}\mu_{\text{layer}}t_{\text{layer}} \quad (1)$$

and

<sup>a)</sup>Electronic mail: oleaariza@fis.ucm.es.

$$\frac{\mu_{\text{impl}}}{R_{S,\text{impl}}} - \frac{\mu_{\text{subs}}}{R_{S,\text{subs}}} = q[n]_{\text{layer}}\mu_{\text{layer}}^2 t_{\text{layer}}, \quad (2)$$

where  $R_{S,\text{impl}}$  and  $\mu_{\text{impl}}$  are the van der Pauw sheet resistance and Hall mobility of the implanted sample;  $R_{S,\text{subs}}$  and  $\mu_{\text{subs}}$  are the van der Pauw sheet resistance and Hall mobility of the substrate; and  $[n]_{\text{layer}}$ ,  $\mu_{\text{layer}}$ , and  $t_{\text{layer}}$  are the carrier concentration, the Hall mobility, and the thickness of the implanted layer, respectively.  $q$  is the electron charge constant. To obtain  $R_{S,\text{subs}}$  and  $\mu_{\text{subs}}$  the implanted layer was stripped. To minimize contact errors, they were covered with photoresist during the etching process. A solution of  $\text{HNO}_3:\text{HF}$  was used to etch away a layer of about 200 nm to ensure that all the Ti implanted was removed from the sample. To measure the etched thickness a Sensofar-Tech S.L. PL  $\mu$  confocal microscope was used.

RBS and channeling-RBS analysis of a sample implanted with a dose of  $10^{15} \text{ cm}^{-2}$  and annealed with an energy density of  $0.8 \text{ J/cm}^2$  and one pulse proved that about 1%–2% of Ti implanted atoms are incorporated into the Si lattice as substitutional ones. SIMS measurements show that about 40% of Ti is lost by the surface when annealing is performed at  $0.8 \text{ J/cm}^2$ . This implies about  $6 \times 10^{14} \text{ cm}^{-2}$  of interstitial Ti and  $10^{13} \text{ cm}^{-2}$  of substitutional Ti, distributed in a 100-nm-thick layer, corresponding to average densities of  $6 \times 10^{19}$  and  $10^{18} \text{ cm}^{-3}$ , respectively. This result means that the solid solubility limit of Ti in Si, which is about  $10^{14} \text{ cm}^{-3}$ , has been widely exceeded.<sup>4</sup> To our knowledge no data of such substitutional quantity of Ti implanted in Si has been reported up to now. Moreover, this quantity of substitutional Ti is, in this case, close to the Mott limit.<sup>5</sup> The remaining Ti in the Si lattice is likely to be located at interstitial positions. Therefore the combination of two nonequilibrium techniques such as ion implantation and laser annealing is a suitable approach to reach the Mott limit of Ti implanted in Si.

Figure 1(a) shows the GIXRD diffractograms for the silicon substrate at different glancing angles. Figures 1(b) and 1(c) show the diffractograms of two representative samples, one of them implanted with the lowest dose ( $10^{15} \text{ cm}^{-2}$ ) and the other one implanted with a high dose ( $10^{16} \text{ cm}^{-2}$ ). Both of them were laser annealed with the highest energy density ( $0.8 \text{ J/cm}^2$ ). No diffraction peaks are presented in the patterns of silicon substrate and in the patterns of the sample implanted with the lowest dose. Then, the reconstruction of the silicon lattice is obtained by means of the laser thermal process for the sample implanted with the lowest Ti dose. For the sample implanted with  $10^{16} \text{ cm}^{-2}$  [Fig. 1(c)], the patterns present two peaks which are attributed to the (220) and (113) reflections of silicon. No peaks associated to TiSi phases are presented. Figure 1(c) also shows that the intensity of the peaks increases with the increase of the glancing angle to  $0.3^\circ$ , and then decreases for higher angles. These results point out the formation of a polycrystalline film of silicon in the implanted region instead of the reconstruction of the original monocrystal silicon lattice. From the GIXRD analysis of the different samples, it is concluded that the samples implanted with a low titanium dose and annealed at a high energy recover their monocrystal

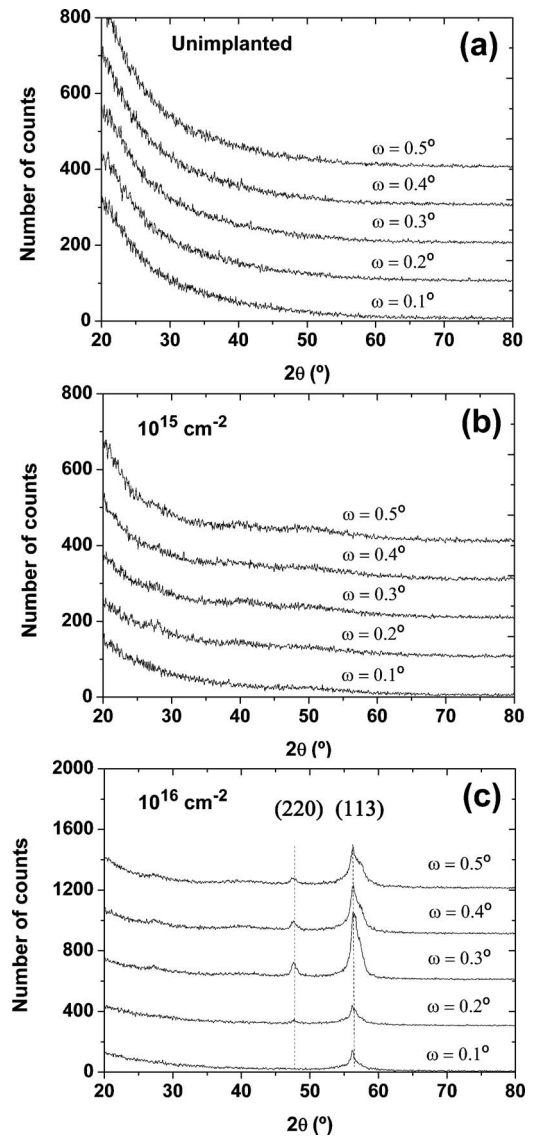


FIG. 1. (a) GIXRD patterns for an unimplanted Si substrate. Measurements were taken at glancing angles  $\omega = 0.1^\circ, 0.2^\circ, 0.3^\circ, 0.4^\circ$ , and  $0.5^\circ$ . (b) GIXRD patterns for a Ti implanted Si sample with  $10^{15} \text{ cm}^{-2}$  and annealed at  $0.8 \text{ J/cm}^2$  with one pulse. Measurements were taken at glancing angles  $\omega = 0.1^\circ, 0.2^\circ, 0.3^\circ, 0.4^\circ$ , and  $0.5^\circ$ . (c) GIXRD spectra of a Ti implanted Si sample with  $10^{16} \text{ cm}^{-2}$  and annealed at  $0.8 \text{ J/cm}^2$  with one pulse. Measurements were taken at glancing angles  $\omega = 0.1^\circ, 0.2^\circ, 0.3^\circ, 0.4^\circ$ , and  $0.5^\circ$ .

structure. However, the samples deposited with higher doses and/or annealed at low laser energy densities present a bad recrystallization since a polycrystalline silicon layer is formed. From this result, the electrical analysis was only performed on samples with the lowest dose and laser annealed with the highest energy density.

Electric measurements proved that all samples have  $n$ -type characteristics. Figure 2 shows the sheet resistance and Hall mobility ( $R_{S,\text{impl}}$  and  $\mu_{\text{impl}}$ ) of a Si sample implanted at 25 keV with a dose of  $10^{15} \text{ cm}^{-2}$  and annealed with an energy density of  $0.8 \text{ J/cm}^2$  and one pulse (blue line). In the same figure the measurements ( $R_{S,\text{subs}}$  and  $\mu_{\text{subs}}$ ) are shown for the same sample after the stripping process of the implanted layer (red line). From these measurements, Hall mobility and carrier concentration of the implanted layer ( $\mu_{\text{layer}}$  and  $[n]_{\text{layer}}$ ) are obtained using the differential Hall method

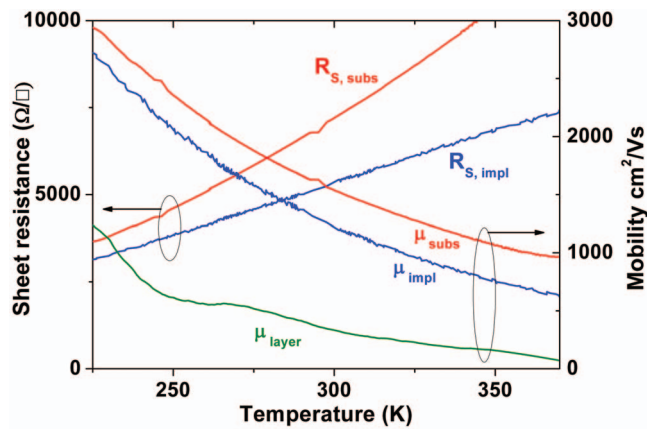


FIG. 2. (Color) Sheet resistance ( $R_{S,impl}$ ) and mobility ( $\mu_{impl}$ ) of a Ti implanted Si sample with  $10^{15} \text{ cm}^{-2}$  and annealed at  $0.8 \text{ J/cm}^2$  with one pulse (blue line). Sheet resistance ( $R_{S,subs}$ ) and mobility ( $\mu_{subs}$ ) of the same stripped sample (red line), and resulting mobility ( $\mu_{layer}$ ) of the stripped layer (green line).

[Eqs. (1) and (2)], which are shown in Fig. 2 ( $\mu_{layer}$ , green line) and Fig. 3 ( $[n]_{layer}$ ). Hall mobility of the implanted layer is about  $400 \text{ cm}^2/\text{V s}$  at room temperature, well above the Hall mobility values measured on  $\text{TiSi}_2$  layers.<sup>9</sup> Therefore, the mobility values shown in Fig. 2 rules out the possibility of  $\text{TiSi}$  metallic compound formation and confirms that the Si lattice damaged in the implantation process is recovered after the annealing process. Although layer mobility is high, there is a reduction of its value in comparison with the expected value for monocrystal Si. This is probably due to the presence of interstitial Ti atoms, according to the RBS analysis, and to the atomic size difference between Ti and Si that increases the electron scattering. Figure 3 shows the Arrhenius plot of the carrier concentration of the implanted layer, obtained by following the procedure previously described. From the slope of this plot, it can be concluded that Ti acts as deep donor level, sited at  $0.21 \pm 0.01 \text{ eV}$  below the conduction band, with an impurity concentration of about  $N_D = 7 \times 10^{17} \pm 2 \times 10^{17} \text{ cm}^{-3}$  and a thermal activation of about 10% at 300 K. This number is far

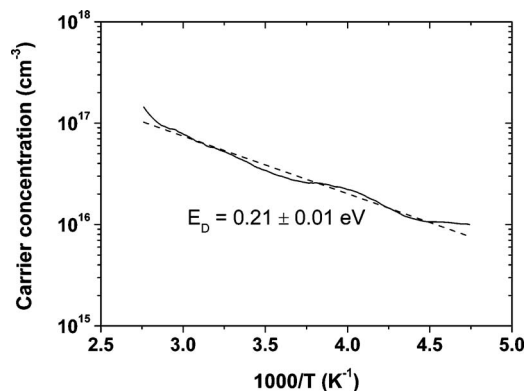


FIG. 3. Arrhenius plot of the carrier concentration ( $[n]_{layer}$ ) of a Ti implanted Si layer with  $10^{15} \text{ cm}^{-2}$  and annealed at  $0.8 \text{ J/cm}^2$  with one pulse (solid line). The linear fit (dashed line) shows a deep level at  $E_D = 0.21 \pm 0.01 \text{ eV}$  below the silicon conduction band.

above the reported solid solubility limit of Ti in Si. A very high activation has never been reported for Ti in Si. Moreover Ti is incorporated substitutionally in concentration near the Mott limit ( $5 \times 10^{19} \text{ cm}^{-3}$ ). Furthermore, the remaining implanted Ti atoms (about  $6 \times 10^{19} \text{ cm}^{-3}$ ), incorporated as interstitials, would reach the Mott limit.

As a concluding remark, we have shown in this communication that Si samples have been effectively implanted with Ti atoms at high doses. The substitutional percentage reached up to 1%–2%, providing a carrier concentration of about  $10^{17} \text{ cm}^{-3}$  at room temperature for the samples with the lowest implantation dose. On the other hand, for the interstitial Ti atoms the Mott limit would be reached. At present, it is an open question if such interstitial Ti atoms have created an IB. A further study is in progress in our laboratory to establish the IB formation unambiguously.

The electrical characterization of implanted samples in the range of temperature analyzed indicated that Ti located at positions different from substitutional ones (for instance, interstitial atoms), did not significantly influence the electrical behavior of the Si implanted layer, which provided high values for the Hall mobility. The substitutional Ti reached values that are close to the Mott transition.

Furthermore, the results shown here present an experimental step toward obtaining of an IB in Si with Ti as doping element. Implanted Ti atoms introduce a deep donor level at  $0.21 \pm 0.01 \text{ eV}$  below the conduction band.

Authors would like to acknowledge the Nanotechnology and Surface Analysis Services of the Universidad de Vigo CACTI for SIMS measurements, the Center for Microanalysis of Materials of the Universidad Autónoma de Madrid for RBS measurements, CAI de difracción de rayos X of the Universidad Complutense de Madrid for GIXRD measurements, and CAI de Técnicas Físicas of the Universidad Complutense de Madrid for ion implantation experiments. This work was made possible thanks to the FPI (Grant No. BES-2005-7063) of the Spanish Ministry of Education and Science. This work was partially supported by the Project NUMANCIA (Grant No. S-0505/ENE/000310) funded by the Comunidad de Madrid and Project GENESIS-FV (Grant No. CSD2006-00004) funded by the Spanish Consolider National Program.

<sup>1</sup>A. Luque and A. Martí, *Phys. Rev. Lett.* **78**, 5014 (1997).

<sup>2</sup>J.-W. Chen, A. G. Milnes, and A. Rohatgi, *Solid-State Electron.* **22**, 801 (1979).

<sup>3</sup>D. Mathiot and S. Hocine, *J. Appl. Phys.* **66**, 5862 (1989).

<sup>4</sup>S. Hocine and D. Mathiot, *Appl. Phys. Lett.* **53**, 1269 (1988).

<sup>5</sup>A. Luque, A. Martí, E. Antolín, and C. Tablero, *Physica B* **382**, 320 (2006).

<sup>6</sup>M. H. Clark, "Laser thermal processing of novel doping schemes in silicon," Ph.D. thesis, University of Florida, 2004.

<sup>7</sup>E. D. Specht, C. J. Sparks, and C. J. McHargue, *Appl. Phys. Lett.* **60**, 2216 (1992).

<sup>8</sup>T. E. Jenkins, *Semiconductor science: growth and characterization techniques* (Prentice Hall, London, 1995), p. 172.

<sup>9</sup>F. Mammoliti, M. G. Grimaldi, and F. La Via, *J. Appl. Phys.* **92**, 3147 (2002).